E. STACHOWSKA, G. SZAWIOŁA, A. BUCZEK, W. KOCZOROWSKI, B. FURMANN, D. STEFAŃSKA, A. WALASZYK, J. DEMBCZYŃSKI

Poznań University of Technology
Chair of Quantum Engineering and Metrology
Poland, e-mail: Gustaw.Szawiola@put.poznan.pl

THE APPLICATION OF LASER-MICROWAVE RESONANCE IN TRAPPED RARE-EARTH IONS TO MAGNETOMETRY

The paper describes an application in magnetometry of an experimental set-up for measurement of hyperfine splittings, constructed in the Chair of Quantum Engineering and Metrology, Poznań University of Technology. A method of determination of magnetic flux density on the basis of the measurement of Zeeman splittings of the hyperfine sublevels of atomic (or ionic) electronic levels is discussed. The experimental setup based on a hyperboloidal Paul trap is presented. A review of the current progress of the work and the results hitherto obtained is given.

Keywords: Paul trap, optical-microwave double resonance, magnetometer, atomic clock, frequency standard

1. INTRODUCTION

The optical-microwave double resonance technique [1] constitutes currently a foundation of the most precise metrological methods. The latest constructions of time and frequency standards, which enable obtaining the relative accuracy of 10^{-16} [2], are based on this technique. Those standards in turn constitute a basis for calibration of other physical quantities, e.g. length or luminosity. A time or frequency unit may in fact be the only fundamental unit of the system of measures, and the units of other physical quantities [3] may be defined as its derivatives. In this context application of a procedure of measurement of the magnetic flux density based on a frequency standard seems quite natural. In magnetometric studies extremely sensitive SQUID detectors [4] are now commonly used. However, methods based on Zeeman splitting of the hyperfine levels [5] and a resonant interaction of atoms or ions with microwave or laser radiation, or with both types of radiation simultaneously [6], are constantly developed. The current Zeeman magnetometers operate in fact as modified frequency standards, with no magnetic field shielding and the possibility of tuning of the optical and microwave frequencies applied to induce relevant transitions in the atoms or ions. Taking into account the sensitivities recently achieved with these devices, which are of the order of $1\mathrm{fT}\cdot\mathrm{Hz}^{-1/2}$ [7,8], we may consider them in certain situations as an alternative for the SQUID based magnetometers; an important advantage of the optical methods of magnetic flux density measurements is that they do not require any cryogenic equipment and allow maintenance of a high precision over a wide range of magnetic fields.

The present work presents an exemplary application of an experimental setup with a qudrupole ion trap, which enables a precise measurement of Zeeman splittings of the hyperfine sublevels of the ground level and low-lying metastable levels of europium isotope $^{151}Eu^{+}$ with a considerable reduction of the time-of-flight broadening. Choice of the ions of this element as a magnetic field "sensor" has been a compromise between the availability of the accurate data on the one side and the attainable wavelengths of laser radiation, generated by the tunable lasers available in our laboratory, as well as the frequency range achievable with the microwave synthesizer.

2. DESCRIPTION OF THE METHOD

The quantitative features of the Zeeman effect, which constitute the basis of the measurement of the magnetic field, presented in this work, are determined with the interactions represented by the components of the Hamiltonian:

$$H_{Zeeman} = H_{hf} + H_B \,. \tag{1}$$

The first component represents the hyperfine interaction (hyperfine structure *hf*) in the absence of the magnetic field, while the second one may be expressed by the formula:

$$H_B = -\vec{\boldsymbol{\mu}}\,\vec{\mathbf{B}}_0 \,. \tag{2}$$

The $\vec{\mathbf{B}}_0$ vector stands for the magnetic flux density under consideration, while the magnetic dipole moment of the atom is defined by the relation:

$$\vec{\boldsymbol{\mu}} = \frac{1}{\hbar}(-g_J \mu_B \vec{\mathbf{J}} + g_I \mu_N \vec{\mathbf{I}}) \,, \tag{3}$$

where the standard [9] handbook denotations for the Planck constant, Bohr magneton, nuclear magneton, total angular momentum of the electron shell and the nuclear spin, as well as the respective Lande factors, have been applied.

In the Eq. (3) an implicit assumption concerning a strong coupling between the spin and the orbital angular momentum of the electron shell into the resultant angular momentum $\vec{\mathbf{J}}$, which is justified for weak magnetic fields. Matrix elements of the operator H_{hf} from (1) are expressed by the following parametric equation [10]:

$$\begin{aligned} &\left\langle IJFM \middle| H_{hf} \middle| IJF'M' \right\rangle = \\ &= \delta_{F,F'}\delta_{M,M'}\left(\frac{K}{2}\, A(J) + \frac{(3/2)K(K+1) - 2I(I+1)J(J+1)}{4I(2I-1)J(2J-1)}\, B(J) \right), \end{aligned} \tag{4}$$

where $K = F(F+1) - I(I+1) - J(J+1)$, and $A(J)$, $B(J)$ denote the hyperfine interaction constants for magnetic dipole and electric quadrupole interactions, respectively. The matrix $\mathbf{H_B}$ can be determined with the use of the formula:

$$\begin{aligned} &\left\langle IJFM \middle| H_B \middle| IJ'F'M' \right\rangle = \delta_{J,J'}\delta_{M,M'}\mu_B\, B_0 \times \\ &\times (-1)^{F-M'+I+1} \begin{pmatrix} F & 1 & F' \\ -M & 0 & M' \end{pmatrix} \sqrt{(2F+1)(2F'+1)} \times \\ &\times \left(g_J (-1)^{J'+F} \sqrt{(2J+1)J(J+1)} \begin{Bmatrix} I & J & F \\ 1 & F' & J' \end{Bmatrix} + \right. \\ &\left. + g_I (-1)^{J+F'} \sqrt{(2I+1)I(I+1)} \begin{Bmatrix} I & J & F \\ F' & 1 & I \end{Bmatrix} \right) \end{aligned} \tag{5}$$

The „matrices” in parenthesis and brackets represent the so-called 3j- and 6j- Wigner coefficients, which numerical values can be obtained with standard functions of the symbolic algebra packages (CAS), e.g. [11].

The quantities directly obtained in the measurement are the microwave frequencies ν corresponding to the eigenvalues of the obtained matrices, i.e. the energy eigenvalues of the atom $\hbar\nu = \left|E_{FM} - E_{FM'}\right|$. The precision of the frequency measurement results from the high quality factor of the electromagnetic resonance transition of the M1 type, induced by the microwave radiation, which yields the population changes of the Zeeman sublevels denoted by the quantum numbers *FM*. As an indicator of these changes the change in laser induced fluorescence intensity is observed in the experiment. The laser wavelength is tuned to the frequency of the resonance E1 transition between the hyperfine sublevels of the levels belonging to configurations of opposite parities. The principle of the double resonance is depicted in Fig. 1.

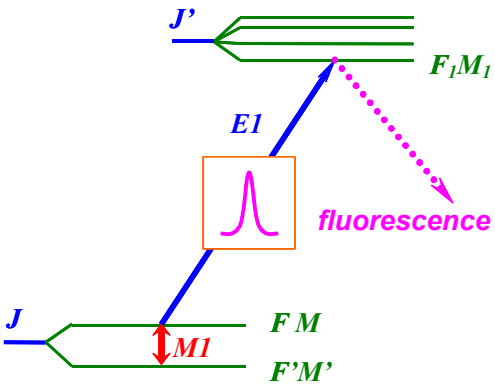

Fig.1. Scheme of the electromagnetic transitions in the method of optical-microwave double resonance.

A review of the formulae (4) and (5) allows to state, that the efficiency of the method described form the point of view of determination of the magnetic flux density relies upon the knowledge of the values of the g_J and g_I factors, as well as the hyperfine structure constants *A*(*J*) and *B*(*J*).

3. EXPERIMENTAL SETUP AND RESULTS

Availability of the literature data concerning europium ion [12, 13, 14], in particular very precisely determined values of the constants *A*(*J*) and *B*(*J*) [12], recently improved accuracy of the measurements of the nuclear Lande factor [13], and the experience with experimental investigations of this element [12, 13] decided on its choice as the magnetic field “detector”. The most important factor has been, however, the appropriate equipment of the laboratory in Chair of Quantum Engineering and Metrology, Poznań University of Technology.

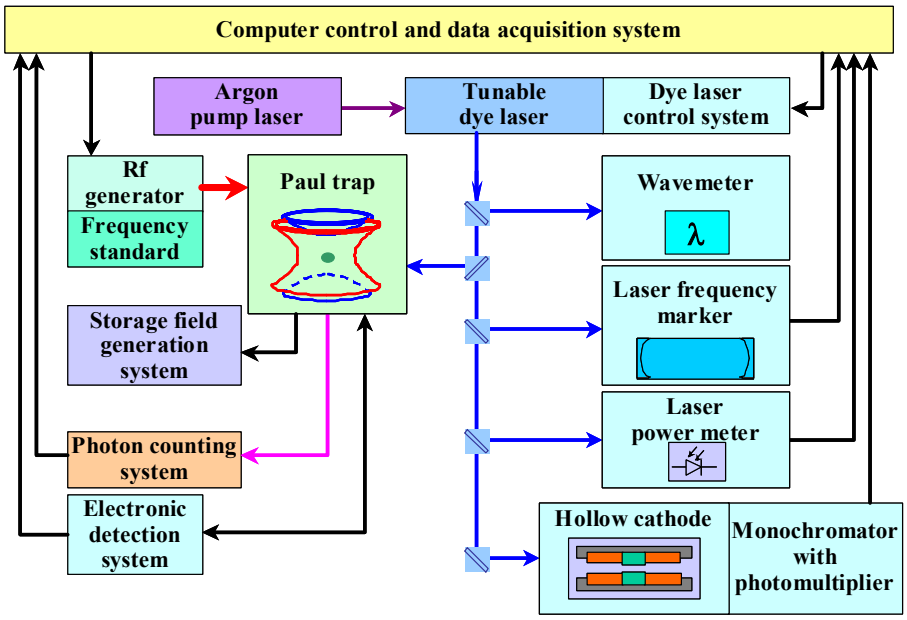

Fig.2. Scheme of the experimental setup.

The experimental setup for investigation of the Zeeman splittings of the hyperfine sublevels, constructed in our laboratory, consists of the following fundamental elements (Fig.2):

- a quadrupole Paul trap with hyperboloidal electrode geometry [15], with a ring electrode diameter $r_0 = 1$cm, placed inside an UHV chamber which allows the achievement of the start pressure $p_{start} = 5 \cdot 10^{-10}$ mbar;
- a system of generation of electromagnetic storage field for the trap: a high voltage generator with a voltage amplitude up to 2kV and the frequency range 390-700kHz (model GAF840814, constructed in the University of Mainz, Germany), a digitally controlled precise DC amplifier capable of generation of the bias voltage of the storage potential up to 100V (constructed in the Institute of Electronics and Telecommunications, Poznań University of Technology);
- a laser system consisting of a tunable single mode ring dye laser (a modified version of the model CR 699-21 of Coherent), optically pumped with an argon ion laser (Spectra Physics, model BeamLok 2085-15-2.5) and operating in the blue-violet spectral range (currently ca. 410-475nm, dye Stilbene 3); the dye laser is equipped with a system of active frequency stabilization; an auxiliary equipment consists of the system of frequency control: a wavemeter (Burleigh WA-1500) and a frequency marker – a confocal Fabry-Perot interferometer with *FSR* = 150MHz (or in some cases *FSR* = 1500MHz);
- a precise microwave radiation synthesizer (Gigatronics, model GT 9000S) with a high stability ($1 \cdot 10^{-9}$/day, $2 \cdot 10^{-10}$/°C), additionally improved with the use of a frequency standard synchronized with a *GPS* signal (model STFS/GPS of the Institute of Electronics and Telecommunications, Poznań University of Technology, with a quartz oscillator of the stability $2 \cdot 10^{-11}$/day);
- a system of detection of the laser induced fluorescence, based on a photomultiplier (Hamamatsu, type R943-02) and a photon counting system (Becker&Hickl, type PHC 322);
- a hollow cathode discharge lamp for the independent recording of the laser induced fluorescence signal of europium ions: this makes the selection of the spectral line and setting of the proper laser operating parameters easier.

The ions of the europium isotope $^{151}Eu^{+}$ have been stored in the buffer gas atmosphere (the buffer gas has been helium of the pressure $5 \cdot 10^{-4}$ mbar) and the following trap operating parameters: the DC signal frequency $f = 600$ kHz, its amplitude $V = 295 \pm 5$V and the bias voltage varied in the range $U = 3\text{-}8$V for the purpose of the electronic detection of the presence of ions in the trap.

The fluorescence signal has been induced with laser radiation of the wavelength of 420.5nm, which corresponds to the transition from the ground level $4f^7(^8S_{7/2})6s\ ^9S_4$ to the excited level $4f^7(^8S_{7/2})6p_{1/2}\ ^9P_3$ with the energy of 23774.28 cm^{-1}. The choice of this transition has allowed to avoid the necessity of frequency doubling of the laser radiation, as was the common practice in earlier works [12, 13], which concerned the measurements of the hyperfine splittings.

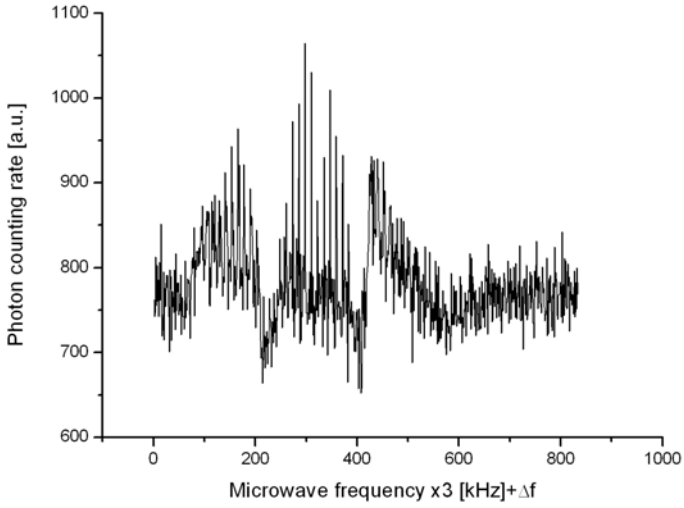

Fig.3. Resonance Zeeman structure (π, σ^- and σ^+) of the transitions $F = 13/2 \leftrightarrow F' = 11/2$; microwave radiation frequency has been scanned stepwise with a step width of 3kHz, the initial frequency value has amounted to $\Delta f = 10016500$kHz.

Under these conditions tuning of the microwave radiation with a step width of 3 kHz allowed observation of the M1 resonances with a distinguished Zeeman structure of the components π, σ^- and σ^+; Fig. 3 represents the recorded spectrum of the transitions between the Zeeman sublevels $F = 13/2 \leftrightarrow F' = 11/2$.

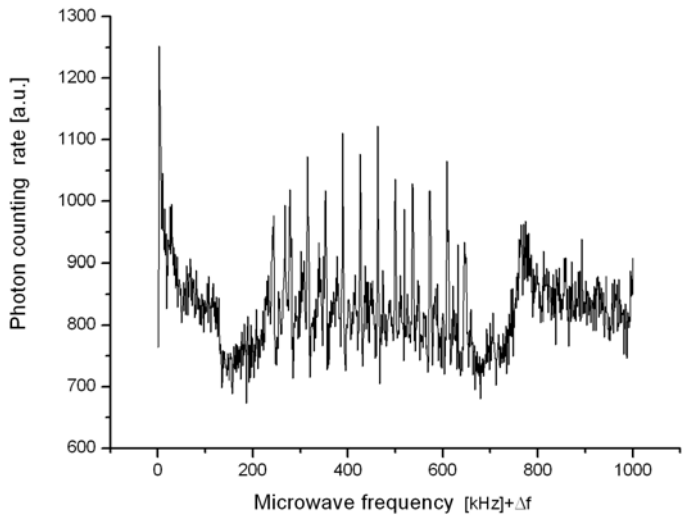

Fig.4. π component of the Zeeman structure of the transitions $F = 13/2 \leftrightarrow F' = 11/2$; microwave radiation frequency has been scanned stepwise with a step width of 1kHz, the initial frequency value has amounted to Δf = 10017000kHz.

A decrease of the frequency increment to 1kHz and the microwave scan range to 1MHz has enabled us to resolve the Zeeman structure of the π components, i.e. recording of all the resonance transitions between the states obeying the selection rule $\Delta M = M - M' = 0$. An example of the recorded signal is presented in Fig. 4.

4. ANALYSIS OF THE RESULTS

A starting point in the analysis of a signal of the kind presented in Fig. 4 are the data concerning europium and the electronic ground state of its ion; the available information is listed in Table 1. There are no experimental data concerning the g_J factor, the quoted value has been determined from the semi-empirical calculations concerning the fine structure [12].

Table 1. Literature data concerning the naturally abundant europium isotopes.

Isotope	^{151}Eu		^{153}Eu	
Atomic mass [amu]	150.919847	[16]	152.921225	[16]
Natural abundance	47.8%	[16]	52.2%	[16]
Nuclear spin	5/2	[16]	5/2	[16]
g_I factor	1.37734(6)	[13]	$(g_I(^{151}\text{Eu})/g_I(^{153}\text{Eu})) = 2.26505(42)$	[15]
g_J factor	1.991169	[12,13]	1.991169	[12,13]
$A(4f^7(^8S_{7/2})6s\ ^9S_4)$[Hz]	1540297394(13)	[17]	684565993(9)	[17]
$B(4f^7(^8S_{7/2})6s\ ^9S_4)$[Hz]	- 660862(231)	[17]	137400(84)	[17]

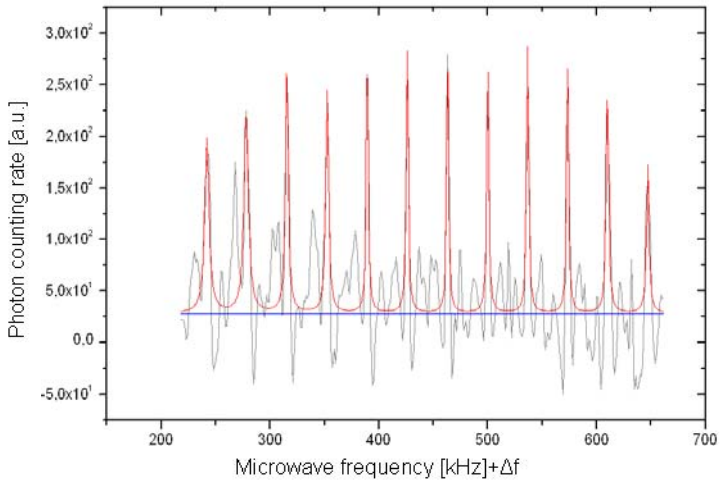

Fig.5. A graphical presentation of the analysis of the signal for the transitions $F = 13/2 \leftrightarrow F' = 11/2$ (π component); microwave radiation frequency has been scanned stepwise with a step width of 1kHz, the initial frequency value has amounted to Δf = 10017000kHz.

The equal values of the nuclear spins, similar values of the atomic masses and the ratio of the nuclear Lande factors close to 2 for the two naturally abundant europium isotopes result in an additional difficulty in the interpretation. As shown in Fig. 5, which depicts the statistical analysis of the resonances observed, resonances of the π component for the isotope ^{151}Eu partially overlap with the σ^+ component for another transition, which cannot be identified unequivocally. Despite the difficulties mentioned the positions of the resonances on the frequency scale can be determined with accuracy better than a half kHz, with an assumption

of Lorentz profiles for the individual peaks. The results obtained for the non compensated magnetic field in the region of ion confinement are listed in Table 2.

Table 2. Relative positions f, halfwidths σ_f and their experimental for resonance transitions; the absolute frequency f can be determined by addition of the shift Δf = 10017000kHz.

i	Transition M=M'	Parameter designation	Parameter value [kHz]	Parameter value error [kHz]	f_i-f_{i-1}
1	M = 11/2	f	241.9	0.4	–
		σ_f	4.8	1.2	
2	M = 9/2	f	278.1	0.4	36.1
		σ_f	4.7	1.0	
3	M = 7/2	f	315.4	0.2	37.3
		σ_f	3.1	0.7	
4	M = 5/2	f	352.43	0.25	37.05
		σ_f	3.2	0.8	
5	M = 3/2	f	389.28	0.18	36.85
		σ_f	2.20	0.55	
6	M = 1/2	f	426.03	0.21	36.76
		σ_f	2.3	0.5	
7	M = -1/2	f	463.1	0.2	37.1
		σ_f	2.05	0.45	
8	M = -2/2	f	500.01	0.23	36.87
		σ_f	2.42	0.56	
9	M = -3/2	f	536.58	0.18	36.57
		σ_f	2.34	0.61	
10	M = -4/2	f	573.3	0.2	36.7
		σ_f	2.2	0.6	
11	M = -5/2	f	609.85	0.25	36.52
		σ_f	2.7	0.7	
12	M = -6/2	f	647.0	0.4	37.2
		σ_f	2.8	1.0	

In order to avoid systematic errors the value of the magnetic flux density has been determined on the basis of the differences of the transition frequencies rather than the absolute frequencies; those differences are listed in the last column of tab.2. Following the discussion of the quadratic Stark effect, the second order Doppler effect and the pressure shift, contained in [17], we can neglect the resulting systematic errors, since they are of the order of 1mHz, 100mHz and 0.5Hz, respectively. The contributions of the second order perturbation theory, resulting from the hyperfine interactions or Zeeman interactions, cannot, however, be neglected [18].

The influence of the dominant second order contributions independent of the magnetic field (magnetic quantum numbers), which introduce corrections into the matrix elements (4), can be ignored, when the determination of B_0 value is based on the frequency differences $f_i - f_{i-1}$ from Table 2. The contribution from the off-diagonal second order effects dependent on B_0 and magnetic quantum numbers, has been taken into account through a direct diagonalization of the described quadratic matrix, obtained in the basis of the order $(2I+1)(2J+1)$ (due to the axial symmetry the calculations are simplified – the matrix is reduced to a submatrix of a lower order). The determination of the magnetic flux density is performed in an iterative loop comprising the following steps:

- diagonalization of the matrix and determination of the eigenvectors,
- parametrization of the expected energy values with the use of the previously determined eigenvectors and a construction of a redundant set of equations concerning the experimentally obtained intervals f_i-f_{i-1},
- calculation of the value of the magnetic flux density with the linear regression method and transferring it to the matrix.

The initial B_0 value can be obtained from the approximate handbook relations [9].

Finally the value of the non compensated magnetic flux density in the center of the trap equal to $B_0 = (31.35 \pm 0.09)\mu T$ has been obtained. This initial result has proved the usefulness of $^{151}Eu^+$ in a standard experimental setup as a magnetic field "sensor", allowing the measurement of the magnetic flux density of the order of a fraction of μT.

5. PERSPECTIVES OF THE FURTHER DEVELOPMENT OF THE METHOD

A natural direction of the development of the presented method, on the experimental side, should consist in the optimization of the experimental setup from the point of view of the measurement sensitivity, in the improvement of the signal-to-noise ratio and in the application of the ions of an element with only one naturally abundant isotope. Further, the method development should be directed at the application of miniature linear traps [19] with a possibility of individually addressing the ions. Such an approach yields the possibility of preparation for the measurement of an ion chain in an entangled state [20]. For a measurement prepared in this way an improvement of the precision, according to [21], proportional to the square of the number of runs, should be expected.

REFERENCES

1. Ertmer W., Hofer B.: *Zero-field hyperfine structure measurements of the metastable states $3d^2 4s\ ^4F_{3/2,9/2}$ of ^{45}Sc using laser-fluorescence atomic-beam-magnetic-resonance technique*. Z. Physik A, vol. 276, no. 1, 1976, pp. 9-14.
2. Holzwarth R., Udem Th., Hänsch T., Knight J., Wadsworth W., Russell P.: *Optical Frequency Synthesizer for Precision Spectroscopy*. Phys. Rev. Lett., vol. 85, no. 11, 2000, pp. 2264-2267.
3. Massalski J., Studnicki J.: *Legal units of measure and physical constants*, Warszawa, Wydawnictwo Naukowe PWN 1999. (in Polish)
4. Nawrocki W., Wawrzyniak M.: *Quantum effects in electrical metrology*, Poznań, Poznań Technical University Publishing House 2003.
5. Schwindt P., Knappe S., Shah V., Hollberg L., Kitching J., Liew L., Moreland J.: *Chip-scale atomic magnetometer*. Appl. Phys. Lett., vol. 85, no. 26, 2004, pp. 6409-6411.
6. Vanier J., Audion C.: *The Quantum Physics of Atomic Frequency Standards*. Bristol and Philadelphia, Adam Hilger 1989.
7. Kominis L., Kornack T., Allerd J., Romalis M.: *A subfemtotesla multichannel atomic magnetometer*. Nature, vol. 422, 2003, pp. 596-599.
8. Budker D., Kimball D., Rochester S., Yashchuk V., Zolotorev M.: *Sensitive magnetometry based on nonlinear magneto-optical rotation*. Phys. Rev. A, vol. 62, no. 4, 2000, pp. 043403(7).
9. Haken H., Wolf H.: *Atoms and quanta. Introduction to contemporary spectroscopy*. Warszawa, Wydawnictwo Naukowe PWN 1997. (in Polish)
10. Lindgren I., Rosen A.: *Relativistic self-consistent field calculations*. Case Stud. At. Phys., vol. 4, 1974, pp. 93-149.
11. Wolfram S.: *The MATHEMATICA® book, 5th ed*. Wolfram Media 2003.
12. Becker O., Enders K., Werth G., Dembczyński J.: *Hyperfine-structure measurements of the $^{151,153}Eu^+$* ground state. Phys. Rev. A, vol. 48, no.5, 1993, pp. 3546-3554.
13. Trapp S., Tommaseo G., Revalde G., Stachowska E., Szawioła G., Werth G.: *Ion trap nuclear resonance on $^{151}Eu^+$*. Eur. Phys. J. D, vol. 26, 2003, pp. 237-244.
14. Evans L., Sandars P., Woodgate G.: *Relativistic effects in many-electron hyperfine structure. III. Relativistic dipole and quadrupole interaction in europium and remeasurement of the nuclear magnetic dipole moments of ^{151}Eu and ^{153}Eu*. Proc. Roy. Soc. A, vol. 289, 1965, pp. 114-121.
15. Major F., Gheorghe V., Werth G.: *Charged particle traps. Physics and techniques of charged particle field confinement*. Berlin, Springer-Verlag 2005.
16. Emsley J.: *Chemistry. Guide on elements.* Warszawa, Wydawnictwo Naukowe PWN 1997. (in Polish)
17. Enders K.: *Hochauflösende Hyperfeinstruktur-Spektroskopie an instabilen Isotopen des Europiums*. Ph.D.Thesis, Universität Mainz 1996.
18. Armstrong L.: *Theory of the Hyperfine Structure of Free Atoms*. New York, Wiley-Interscience 1971.

19. Stick D., Hensinger W., Olmschenk S., Madsen M., Schwab K., Monroe C.: *Ion trap in a semiconductor chip*. Nature Physics, vol. 2, 2005, pp. 36-39.
20. Häffner H., Hänsel W., Roos C., Benhelm J., Chek-al-kar D., Chwalla M., Körber T., Rapol U., Riebe M., Schmidt P., Becher C., Gühne O., Dür W., Blatt R.: *Scalable multiparticle entanglement of trapped ions*. Nature, vol. 438, 2005, pp. 643-646.
21. Giovannetti V., Lloyd S., Maccone L.: *Quantum Metrology*. Phys. Rev. Lett. B, vol. 96, no. 1, 2006, pp. 010401(4).

ZASTOSOWANIE REZONANSU LASEROWEGO-MIKROFALOWEGO UWIĘZIONYCH JONÓW

Streszczenie

Praca przedstawia postęp prac w zastosowaniu w magnetometrii stanowiska doświadczalnego do pomiaru rozszczepień nadsubtelnych, zbudowanego w Katedrze Inżynierii i Metrologii Kwantowej Politechniki Poznańskiej. Do detekcji pola magnetycznego wykorzystano uwięzione w pułapce Paula jony izotopu europu $^{151}Eu^{+}$. Wartość pola magnetycznego wyznaczano w prezentowanej metodzie w oparciu o przejścia rezonansowe M1 między stanami zeemanowskimi podpoziomów nadsubtelnych $F = 13/2$ i $F = 11/2$ podstawowego poziomu $4f^{7}(^{8}S_{7/2})6s\ ^{9}S_{4}$ stosowanego pierwiastka. O dostrojeniu do rezonansu świadczyła zmiana natężenia fluorescencji indukowanej światłem laserowym o długości fali 420,5nm. Wykorzystanie tego przejścia jest istotnym novum metody, pozwalającym na wykorzystanie konwencjonalnego barwnikowego lasera, bez konieczności generacji drugiej harmonicznej. Ponadto zaangażowanie w pomiarach stanów o relatywnie dużej liczbie kwantowej *F*, co było możliwe w przypadku europu, pozwoliło wyznaczyć wartość indukcji magnetycznej z wykorzystaniem aż dwunastu precyzyjnie zmierzonych wartości częstości rezonansowych. Poprawia to wiarygodność uzyskanych wyników i stanowi o zalecie stosowanej metody. W pomiarach odnoszono się do wzorca częstości (model STFS/GPS, Instytutu Elektroniki i Telekomunikacji PP) z podwójnie termostatowanym oscylatorem kwarcowym, stabilizowanym sygnałem *GPS*. W analizie statystycznej bezpośrednich wyników pomiaru i ich interpretacji wykorzystano iteracyjną metodę diagonalizacji macierzy hamiltonianu umożliwiającą uwzględnienie dominujących efektów II rzędu rachunku zaburzeń – przyczynków zależnych od kwadratu i wyższych potęg wartości indukcji magnetycznej. Krótko dyskutowana jest metoda eliminacji potencjalnych systematycznych błędów pomiaru i interpretacji otrzymanych wyników. Ostatecznie zaprezentowano przykładowy pomiar indukcji pola magnetycznego z precyzją lepszą niż 100nT, z możliwością istotnej poprawy po optymalizacji wzbudzania jonów i detekcji fotonów.